Electronic Supplementary Material (ESI) for Journal of Materials Chemistry A.

Electronic Supplementary Information for

Origin of Excellent Rate and Cycle Performance of Sn_4P_3 Binary Electrode for Sodium-Ion Battery†

Sung Chul Jung,[a] Jin-Ho Choi,[b] and Young-Kyu Han*[b]

[a]Department of Physics, Pukyong National University, Busan 48513, Republic of Korea

[b]Department of Energy and Materials Engineering and Advanced Energy and Electronic Materials Research Center, Dongguk University-Seoul, Seoul 100-715, Republic of Korea

*Corresponding author

E-mail address: ykenergy@dongguk.edu (Y.-K. Han).

Atomic structures

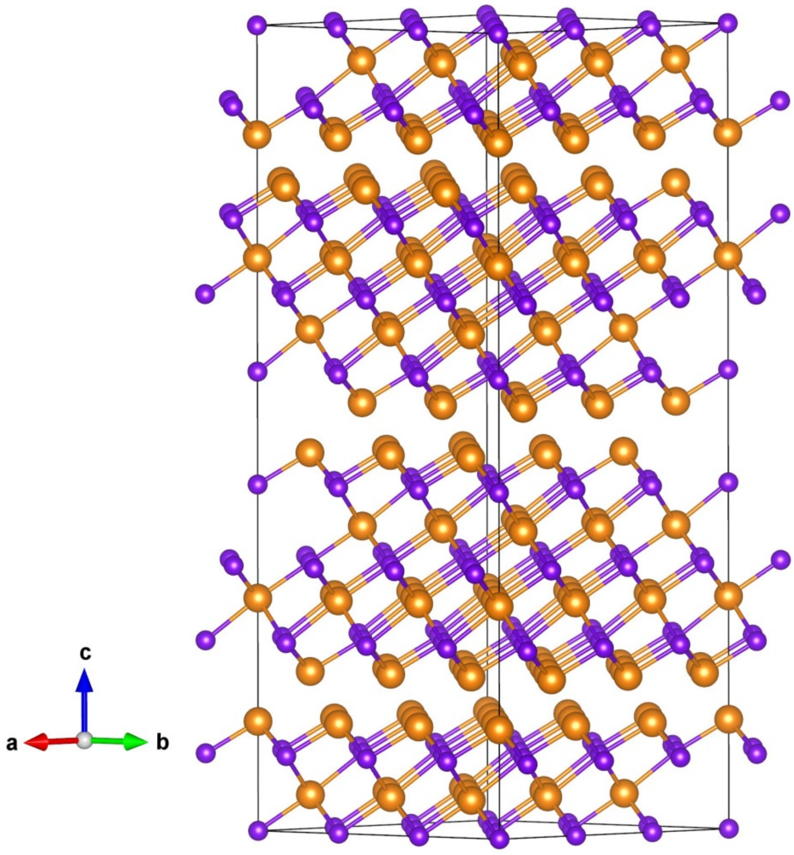

Fig. S1 Optimized structure of *c*-Sn_4P_3. Orange and purple balls represent the Sn and P atoms, respectively.

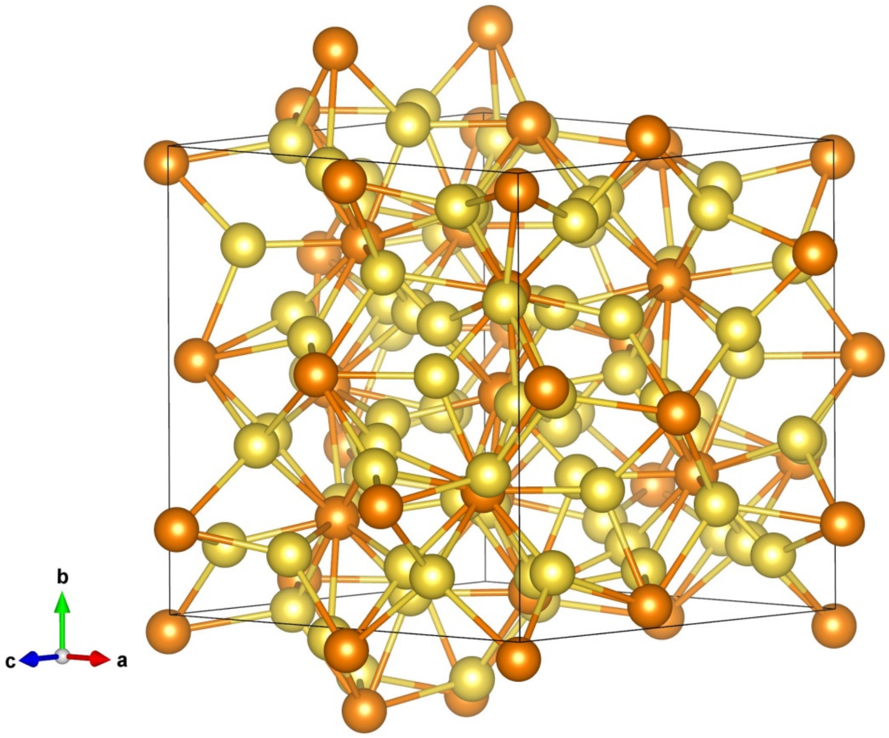

Fig. S2 Optimized structure of *c*-$Na_{15}Sn_4$. Yellow and orange balls represent the Na and Sn atoms, respectively.

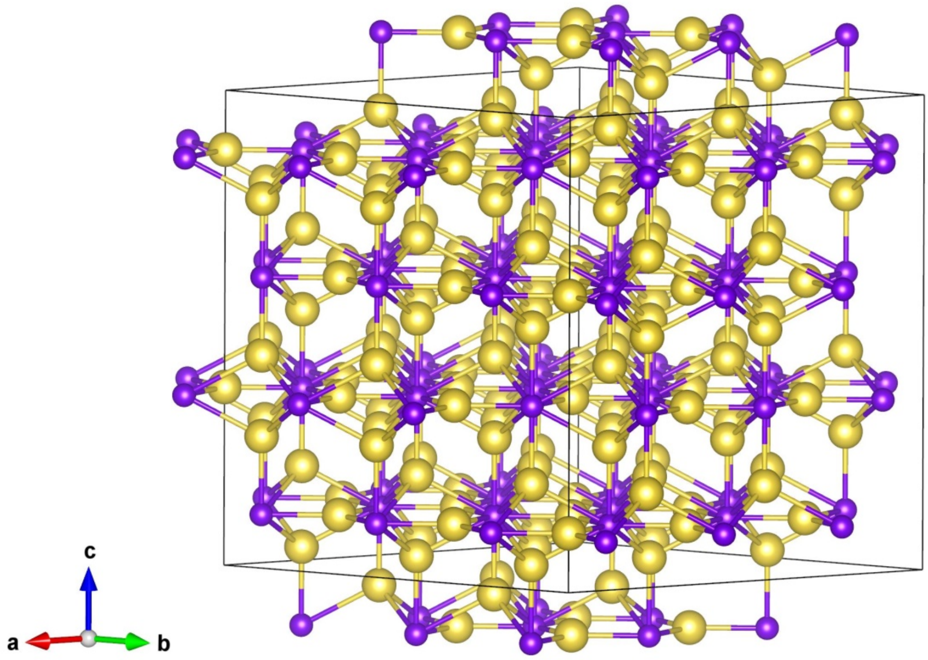

Fig. S3 Optimized structure of *c*-Na_3P. Yellow and purple balls represent the Na and P atoms, respectively.

a-Sn_4P_3	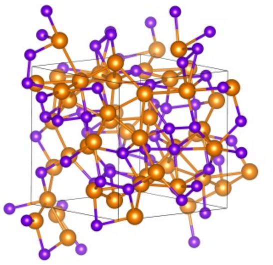	*a*-$Na_4Sn_4P_3$	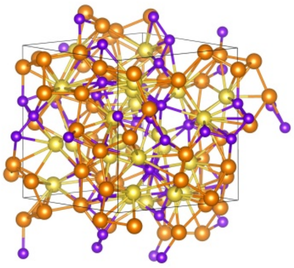
a-$Na_8Sn_4P_3$	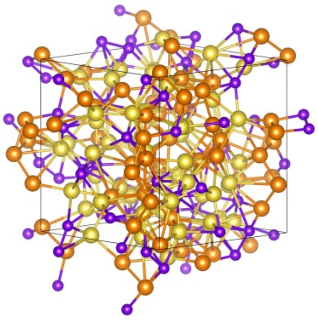	*a*-$Na_{12}Sn_4P_3$	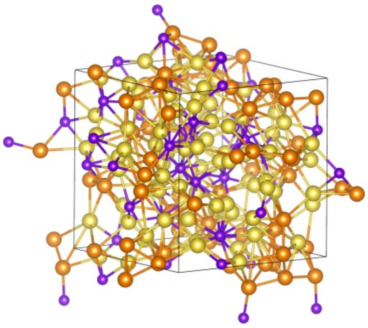
a-$Na_{16}Sn_4P_3$	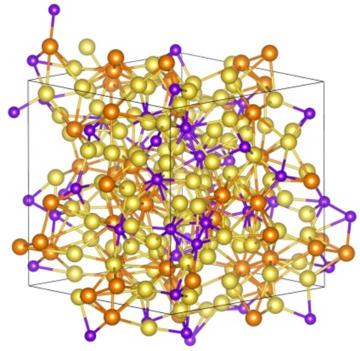	*a*-$Na_{20}Sn_4P_3$	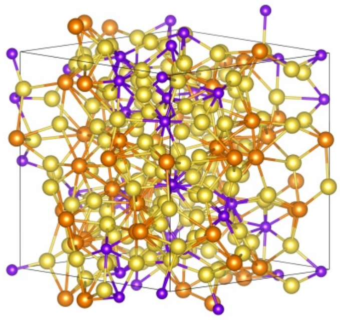
a-$Na_{24}Sn_4P_3$	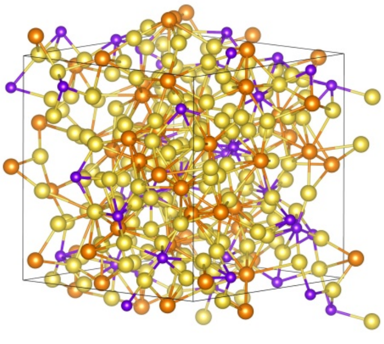	*a*-$Na_{28}Sn_4P_3$	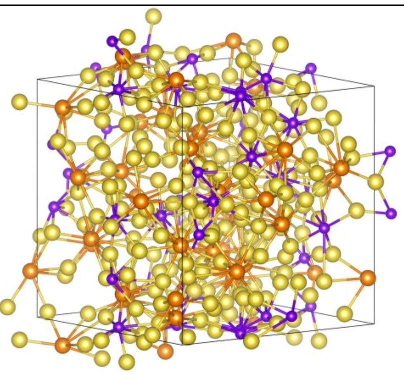

Fig. S4 Optimized structures of *a*-$Na_xSn_4P_3$ (x = 0, 4, 8, 12, 16, 20, 24, and 28). Yellow, orange, and purple balls represent the Na, Sn, and P atoms, respectively.

Voltages

We calculated the average voltages of *a*-$Na_xSn_4P_3$ using not only the PBE functional but also the HSE06 functional. We found that the voltage curve calculated by the HSE06 functional is very similar to that calculated by the PBE functional (Fig. S5). This can be understood from the fact that the voltage is defined as the derivative of total energy with respect to *x*. The absolute energies can vary depending on the used functional, but the variation of energies with *x* does not significantly depend on the functional. As a result, despite its inaccuracy in describing band gap, the PBE functional has similar accuracy in describing voltage as the hybrid functional. Indeed, the calculated voltage curve using the PBE functional lies between the experimental charge–discharge profiles, as shown in Fig. 2b.

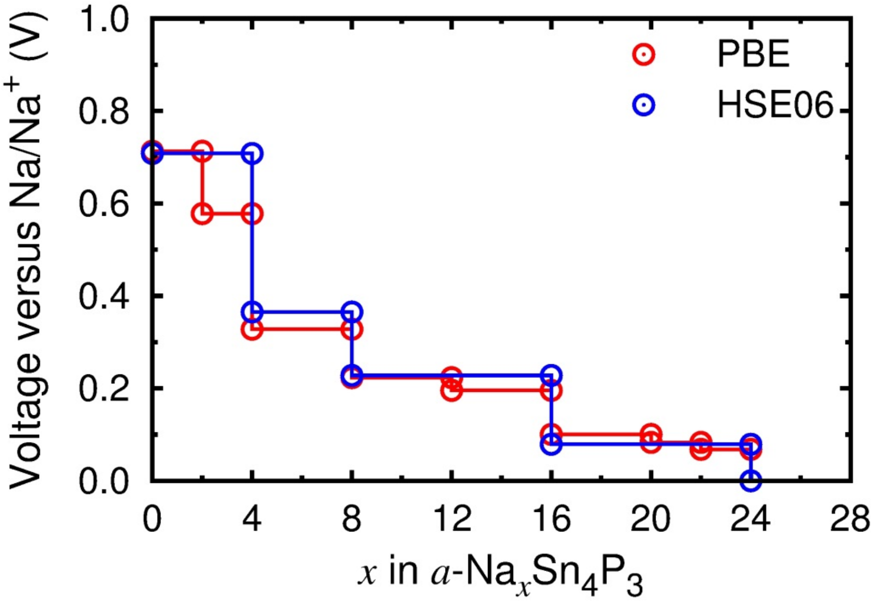

Fig. S5 Average voltages of *a*-$Na_xSn_4P_3$, calculated by the PBE and HSE06 functionals.

Bulk moduli

Bulk modulus is defined as $B = V_0(\partial^2 E_{tot}/\partial V^2)$, where E_{tot} is the total energy of unit cell, V_0 is the equilibrium volume of unit cell, and V is the volume of unit cell. The total energies of *a*-$Na_{15}Sn_4$ and *a*-Na_3P were calculated as a function of volume (Fig. S6) and were fitted to Murnaghan's equation of state to determine their bulk moduli.

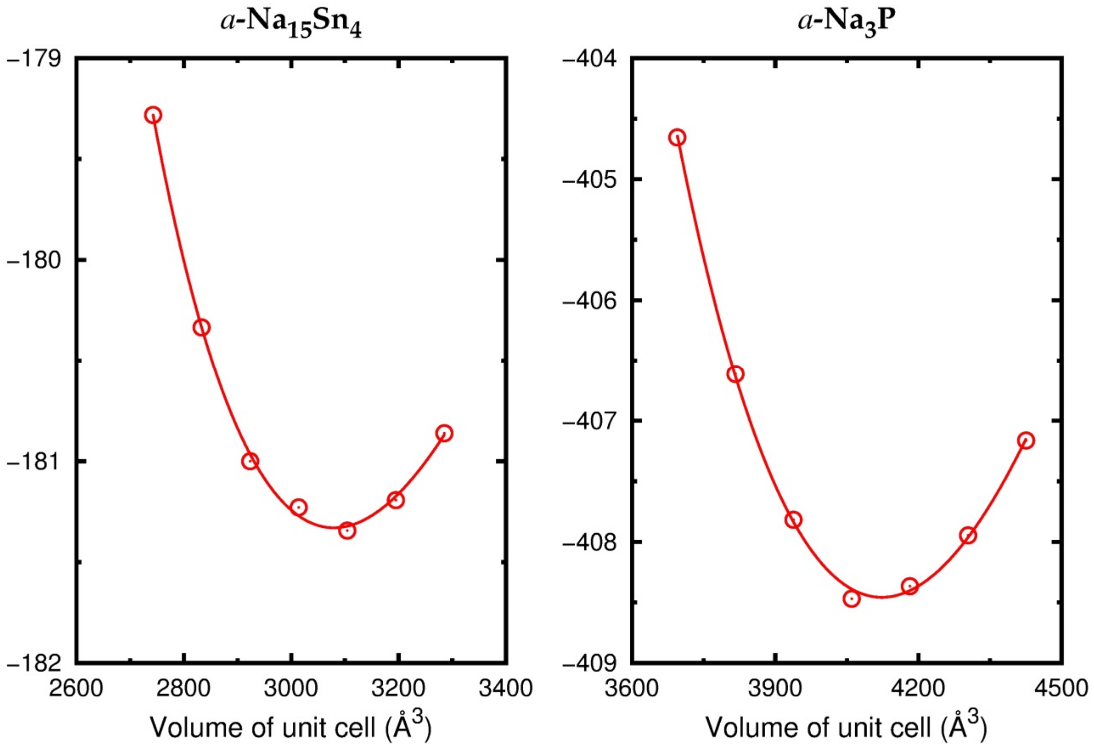

Fig. S6 Total energies of *a*-$Na_{15}Sn_4$ and *a*-Na_3P as a function of the volume of unit cell.

Diffusivities

The self-diffusion coefficients *D* of Na atoms in of *a*-$Na_{1.33}Sn_4P_3$, *a*-$Na_{24}Sn_4P_3$, *a*-$Na_{15}Sn_4$, and *a*-Na_3P at $T = 300$ K were obtained from the Einstein relation $\langle r^2(t)\rangle = 6Dt$ where $\langle r^2\rangle$ is the mean square displacement. We calculated the $\langle r^2\rangle$ values of Na atoms from the AIMD simulations for 10 ps at $T = 1200$, 1600, 2000, and 2400 K and then determined the *D* values at each temperature. The determined *D* values at these high temperatures were used to extrapolate the *D* value at $T = 300$ K using the Arrhenius law $D = D_0 \exp(-E_D/k_BT)$ where D_0 is the pre-exponential factor, E_D is the activation energy for diffusion, and *k* is the Boltzman constant. Temperature dependences of Na diffusivities are shown in Fig. S7.

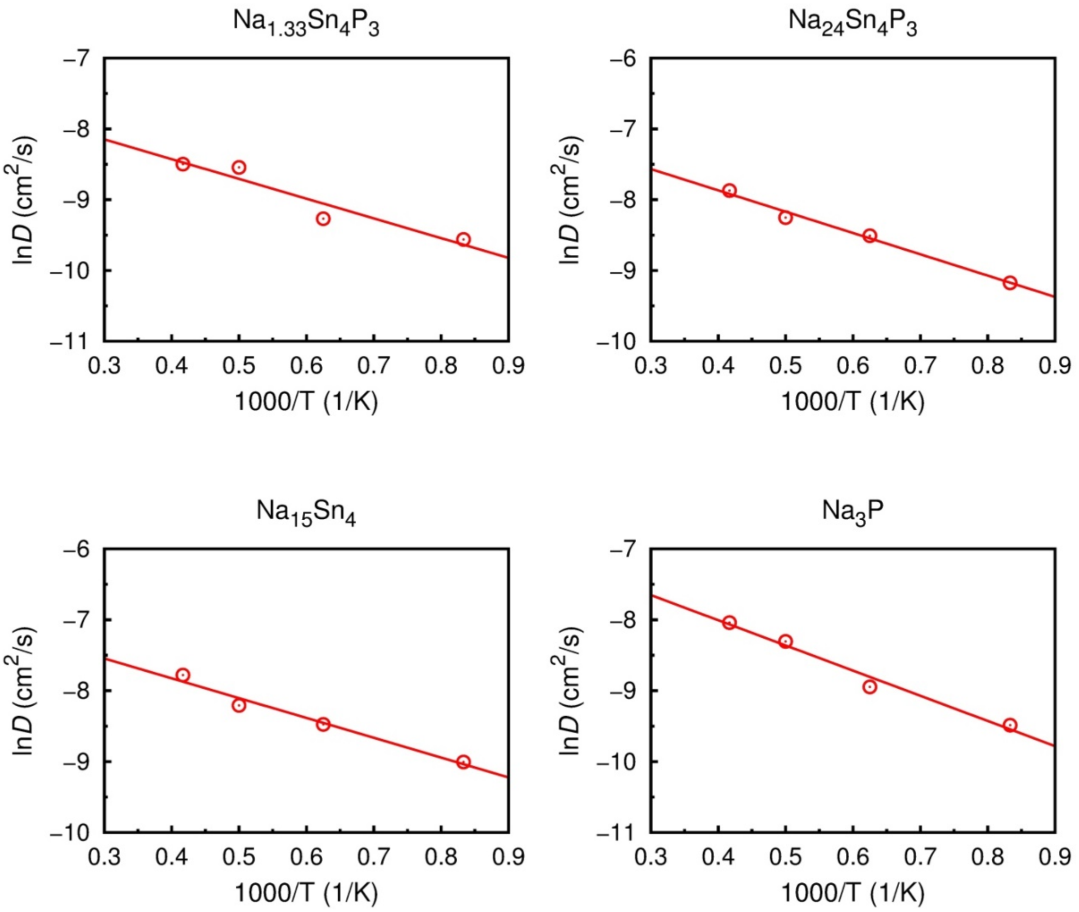

Fig. S7 Temperature dependences of Na diffusivities in *a*-Na$_{1.33}$Sn$_4$P$_3$, *a*-Na$_{24}$Sn$_4$P$_3$, *a*-Na$_{15}$Sn$_4$, and *a*-Na$_3$P.

Structural analyses

We analyzed the average partial coordination numbers (CN) of Na, Sn, and P in a-$Na_{1.33}Sn_4P_3$, a-$Na_{24}Sn_4P_3$, a-$Na_{15}Sn_4$, and a-Na_3P and radial distribution functions (RDF) for the Na–Na, Na–Sn, Na–P, Sn–Sn, P–P, and Sn–P pairs in a-$Na_xSn_4P_3$. The analyses were done for the equilibrium structures, i.e., the room-temperature simulation structures during the final MD step in the procedure for constructing the amorphous phases. The CN and RDF were obtained using the RINGS code [Roux and Jund, Comput. Mater. Sci. 49 (2010) 70] and were presented in Table S1 and Fig. S8, respectively.

Table S1

Partial coordination numbers of Na, Sn, and P in *a*-$Na_{1.33}Sn_4P_3$, *a*-$Na_{24}Sn_4P_3$, *a*-$Na_{15}Sn_4$, and *a*-Na_3P. The bond cutoff distances are 4.6, 4.5, 4.2, 3.6, 3.3, and 2.5 Å for the Na–Na, Na–Sn, Na–P, Sn–Sn, Sn–P, and P–P bonds, respectively, which correspond to the first-minimum positions of the RDFs (Fig. S8).

	a-$Na_{1.33}Sn_4P_3$	*a*-$Na_{24}Sn_4P_3$	*a*-$Na_{15}Sn_4$	*a*-Na_3P
$CN_{Na–Na}$	2.10	10.31	9.89	11.04
$CN_{Na–Sn}$	6.93	1.89	2.90	
$CN_{Na–P}$	4.55	1.18		3.27
$CN_{Sn–Na}$	2.31	11.37	10.90	
$CN_{Sn–Sn}$	3.01	0.52	0.79	
$CN_{Sn–P}$	1.75	0.04		
$CN_{P–Na}$	2.02	9.47		9.82
$CN_{P–Sn}$	2.34	0.05		
$CN_{P–P}$	1.11	0.00		0.24

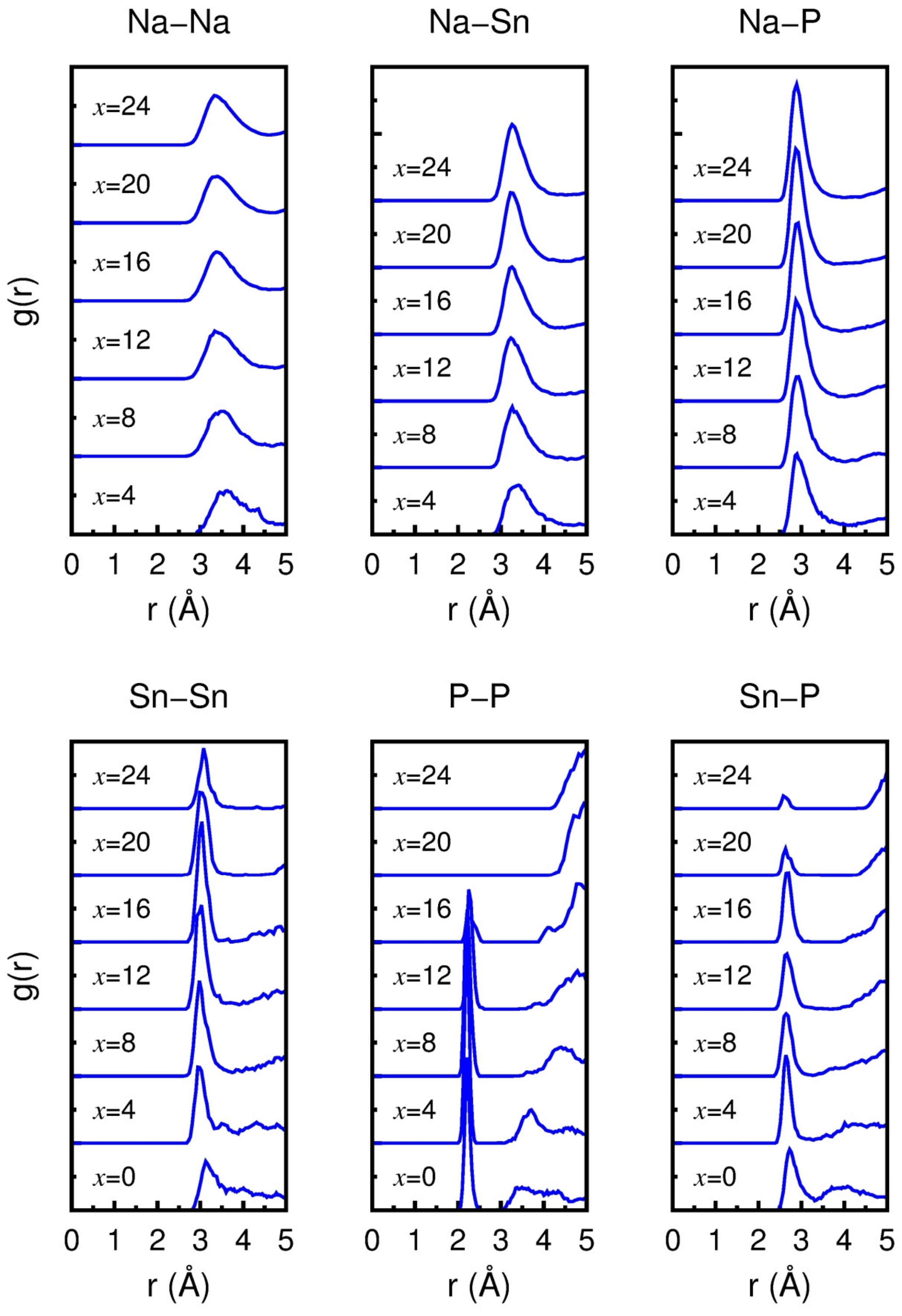

Fig. S8 Radial distribution functions for the Na–Na, Na–Sn, Na–P, Sn–Sn, P–P, and Sn–P pairs in *a*-$Na_xSn_4P_3$.

Table S2

Partial coordination numbers of Na, Sb, and P in *a*-Na_6SbP, *a*-Na_3Sb, and *a*-Na_3P. The bond cutoff distances are 4.6, 4.5, 4.2, 3.6, 3.3, and 2.5 Å for the Na–Na, Na–Sb, Na–P, Sb–Sb, Sb–P, and P–P bonds, respectively.

	a-Na_6SbP	*a*-Na_3Sb	*a*-Na_3P
$CN_{Na–Na}$	10.13	9.00	11.04
$CN_{Na–Sb}$	1.82	3.30	
$CN_{Na–P}$	1.50		3.27
$CN_{Sb–Na}$	10.95	9.91	
$CN_{Sb–Sb}$	0.00	0.06	
$CN_{Sb–P}$	0.00		
$CN_{P–Na}$	9.00		9.82
$CN_{P–Sb}$	0.00		
$CN_{P–P}$	0.65		0.24